

## Waveguide fabrication and high-speed in-line intensity modulation in 4-N,N-4'-dimethylamino-4'-N'-methyl-stilbazolium tosylate

F. Pan, K. McCallion, and M. Chiappetta

Citation: *Appl. Phys. Lett.* **74**, 492 (1999); doi: 10.1063/1.123956

View online: <http://dx.doi.org/10.1063/1.123956>

View Table of Contents: <http://apl.aip.org/resource/1/APPLAB/v74/i4>

Published by the [American Institute of Physics](http://www.aip.org).

---

### Related Articles

Bloch surface waves-controlled fluorescence emission: Coupling into nanometer-sized polymeric waveguides  
*APL: Org. Electron. Photonics* **5**, 39 (2012)

Bloch surface waves-controlled fluorescence emission: Coupling into nanometer-sized polymeric waveguides  
*Appl. Phys. Lett.* **100**, 063305 (2012)

Periodically focused modes in chains of dielectric spheres  
*Appl. Phys. Lett.* **100**, 061123 (2012)

Enhanced spontaneous emission from quantum dots in short photonic crystal waveguides  
*Appl. Phys. Lett.* **100**, 061122 (2012)

Transmission enhancement in a non-adiabatic tapered nano-aperture waveguide  
*Appl. Phys. Lett.* **100**, 051104 (2012)

---

### Additional information on *Appl. Phys. Lett.*

Journal Homepage: <http://apl.aip.org/>

Journal Information: [http://apl.aip.org/about/about\\_the\\_journal](http://apl.aip.org/about/about_the_journal)

Top downloads: [http://apl.aip.org/features/most\\_downloaded](http://apl.aip.org/features/most_downloaded)

Information for Authors: <http://apl.aip.org/authors>

## ADVERTISEMENT



# Waveguide fabrication and high-speed in-line intensity modulation in 4-*N,N*-4'-dimethylamino-4'-*N'*-methyl-stilbazolium tosylate

F. Pan,<sup>a)</sup> K. McCallion, and M. Chiappetta

*Molecular OptoElectronics Corporation (MOEC), 877 25th Street, Watervliet, New York 12189*

(Received 14 August 1998; accepted for publication 18 November 1998)

We report the formation of thin-film waveguides of organic crystals by precision optical polishing and the fabrication of an electro-optic intensity modulation device based on a thin-film waveguide of *N,N*-4'-dimethylamino-4'-*N'*-methyl-stilbazolium tosylate (DAST<sup>®</sup>) as an overlay on a side-polished fiber (SPF). Successful fabrication of single-crystal DAST<sup>®</sup> waveguides with thicknesses in the 20–25  $\mu\text{m}$  range have been produced. The waveguides were investigated via an evanescent coupling technique using side-polished fibers rather than traditional end-firing methods. Surface quality is believed to have been sufficient for low-loss propagation. Electrodes were added to the SPF/DAST<sup>®</sup> overlay architecture and intensity modulation observed out to 18 GHz. The device frequency response is believed to extend beyond 100 GHz under optimum conditions.

© 1999 American Institute of Physics. [S0003-6951(99)02704-7]

Fiber-optic communication systems take advantage of large signal bandwidth availability and low signal attenuation. As these systems develop, external modulation of a high-power continuous-wave (cw) laser source is becoming the preferred method of impressing rf signal information onto the optical carrier, particularly with the shift towards 10 Gb/s speeds and beyond. A considerable research effort has been directed at the development of high-speed modulators, with much success in particular using LiNbO<sub>3</sub>,<sup>1–3</sup> while impressive electro-optic polymer and III–V multi-quantum-well semiconductor devices have also emerged.<sup>4,5</sup> Each material and device design offers certain advantages but there remain several trade offs in terms of insertion loss, frequency response, modulation sensitivity, and cost.

The basic criteria for high-performance electro-optic modulators are large electro-optic modulation bandwidth and low-power drive requirements. They are dominated by the properties of electro-optic materials, such as electro-optic coefficients, dielectric constants, transparency, and linear refractive index. Inorganic ionic electro-optic crystals, such as LiNbO<sub>3</sub>, have been well investigated and developed for applications. The 3 dB bandwidth of a bulk modulator (frequency at which the power in the optical sidebands is reduced by one half) is 6.7 GHz for a 1 cm LiNbO<sub>3</sub> crystal, and a figure of merit ( $n^7 r_{\text{eff}}^2 / \epsilon$ ) for a minimum drive power required is  $6.0[\times 10^3 (\text{pm/V})^2]$  at 1300 nm. DAST<sup>®</sup> crystals have the largest second-order nonlinear optical (NLO) coefficients, e.g.,  $d_{11} = 1010 \pm 110$  pm/V at 1318 nm,<sup>6</sup> the electro-optic coefficients, e.g.,  $r_{11} = 50 \pm 5$  pm/V at  $\lambda = 1313$  nm.<sup>7</sup> Additionally, the low dielectric constants (e.g.,  $\epsilon_{11} = 5.2$ ) of DAST<sup>®</sup> crystal is an additional advantage for high-speed electro-optic modulation.<sup>7,8</sup> At  $\lambda = 1313$  nm, which is an interesting wavelength for optic communication, DAST<sup>®</sup> crystals provide a 140 GHz bandwidth for a 1 cm crystal, and a figure of merit of  $130[\times 10^3 (\text{pm/V})^2]$ .<sup>9</sup> In conclusion, the large electro-optic coefficients, high modulation band-

widths, and low-power consumption of DAST<sup>®</sup> crystals are advantageous for fast electro-optical modulation.

Waveguide fabrication of organic NLO crystals is required to produce efficient devices suitable for integrated optics and fiber-optical communications. Many researchers have reported organic crystal waveguide formation via growth methods, such as the growth of organic thin-film crystals between two flat substrates. However, there are many technical difficulties to be solved. These include the control of single-crystal growth without spontaneous nucleation, control of the crystallographic orientation of thin-film crystals, growth of thin-film crystals with high optical quality, and increased growth speed of thin films. In this work we report the formation of thin-film waveguides of organic crystals by precision optical polishing and the fabrication of an electro-optic intensity modulation device based on a DAST<sup>®</sup> thin-film waveguide as an overlay on a side-polished fiber (SPF).

Anhydrous DAST<sup>®</sup> crystals belong to the monoclinic space group *Cc*, and the melting point of the crystal is 256 °C. DAST<sup>®</sup> single crystals were grown from a seeded, saturated methanol solution by controlled lowering of the temperature at a rate of 0.1–0.2 °C/day.<sup>10</sup> The crystals normally grew as *c* plates (see Fig. 1). The polar axis of the crystal is along  $x_1$ . For the electro-optic modulators, single crystals of DAST<sup>®</sup> were cut into *c*-plate samples with dimen-

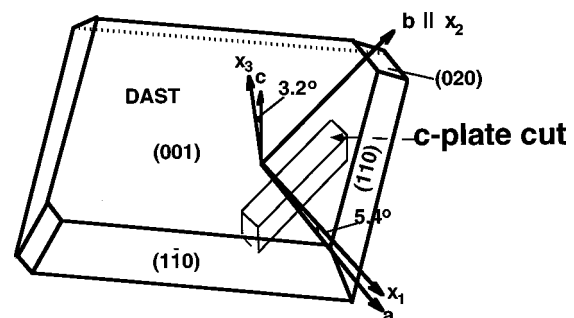


FIG. 1. Directions of DAST crystal grown and *c* plate cut.

<sup>a)</sup>Electronic mail: pan@moe.com

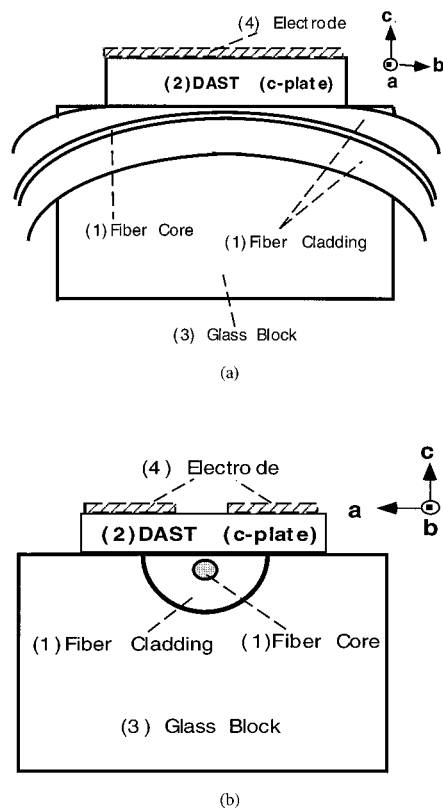


FIG. 2. The SPF/DAST<sup>®</sup>-overlay modulator structure (a) sideview; (b) cross section.

sions of up to about  $a \times b \times c = 3 \times 7(2) \times 1 \text{ mm}^3$  (see Fig. 1). The optical samples were prepared by polishing of the  $c$  faces. Polarized microscopy investigations showed that these samples were homogeneous without cracks or solvent inclusions in the crystal. Furthermore, interference pictures showed that the optical surfaces were flat to about  $\lambda/4 - \lambda/2$  ( $\lambda = 580 \text{ nm}$ ), and also confirmed the excellent optical quality of the polished surface.

The SPF/overlay waveguide architecture allows device implementations which offer the advantages of low insertion loss, zero backreflection, simple device interfacing, and the use of a variety of active materials.<sup>11</sup> When thin nonlinear optical crystals are fabricated as the overlay waveguide, the device architecture can be used for electro-optic modulation, tunable filtering, parametric amplification, and frequency conversion. The basic geometry of the SPF/DAST<sup>®</sup> overlay waveguide device consists of four main components (see Fig. 2): (1) a single-mode optical fiber, side-polished close to the core, (2) a high index, planar multimode overlay waveguide comprised of a thin, polished DAST<sup>®</sup>  $C$  plate, (3) a fused silica substrate block with a controlled radius groove for locating the fiber and supporting the overlay waveguide, and (4) an electrode structure patterned on the top surface of the thin DAST<sup>®</sup>  $C$ -plate waveguide.

The basic principle of operation of the device relies on evanescent coupling between the single mode of the optical fiber and the planar multimode DAST<sup>®</sup> waveguide. When phase matching of the propagation constant of the single fiber mode and that of a mode of the multimode overlay DAST<sup>®</sup> waveguide is established, strong coupling of power from the fiber to the overlay DAST<sup>®</sup> waveguide occurs. The

phase-matching situation can be altered by inducing a refractive index change in the DAST<sup>®</sup> waveguide. Such a refractive index change in the DAST<sup>®</sup> waveguide can be achieved via the application of an electric field along the  $x_1$ -dielectric axis, leading to an electro-optic device response. Due to the strong modal wavelength dispersion exhibited by the DAST<sup>®</sup> multimode waveguide, a series of phase-matching conditions occur as the input wavelength to the device is varied. This results in a periodic-like channel dropping filter response. The wavelength location of each dropped channel (or resonance) depends on the material (core) index, thickness, and superstrate index of the overlay waveguide. Changing the overlay material index (e.g., via an electro-optic effect) causes a corresponding shift in the device spectral response. Thus, by tuning a spectral resonance (channel) to coincide with a fixed narrowline laser source, the device can be used for electro-optic intensity modulation.<sup>11,12</sup>

A standard single-mode optical fiber (Corning SMF-28) was used with a core region of  $8.3 \mu\text{m}$  and a cladding of  $125 \mu\text{m}$ . The fiber is fixed in a groove cut in a silica block with fixed curvature. The fiber cladding and the block surface were lapped and polished down close to the fiber core to gain access to the evanescent field of the fiber mode. The polished  $c$  plates were bonded onto the side polished fiber with a low-index, low-viscosity UV glue or epoxy. The  $a$  axis ( $x_1$  axis) of the  $c$  plate was orientated normal to the fiber core (see Fig. 2). Then, the upper face of the DAST<sup>®</sup>  $c$  plate was lapped and polished until it was reduced to a thin film. Since DAST<sup>®</sup>, which is an organic crystal, tends to be mechanically weak, the crystal cracks very easily as it is thinned, such as below a  $100 \mu\text{m}$  thickness. However, by carefully controlling the pressure of lapping and polishing to minimize the induced stress, the DAST<sup>®</sup>  $c$  plates were polished down to thin films with thickness about  $20\text{--}25 \mu\text{m}$ . The thin crystals of DAST<sup>®</sup> then behave as the planar multimode overlay waveguide in the device. Transverse-electric (TE) polarization is parallel to the  $x_1$ -dielectric axis, while transverse-magnetic (TM) polarization is parallel to the  $x_3$ -dielectric axis. There are strong birefringence effects along the  $x_1$  and  $x_3$  axes due to the large difference between their refractive indices, such as  $n_1 = 2.18$  and  $n_3 = 1.60$  at  $\lambda = 1.3 \mu\text{m}$ , respectively.

A test device with a DAST<sup>®</sup> overlay thickness of  $25 \mu\text{m}$  was characterized in the  $1300 \text{ nm}$  spectral region. Light from a  $1300 \text{ nm}$  light-emitting diode (LED) was passed through a polarizer and polarization controller and launched into the SPF/DAST<sup>®</sup> device. This allowed precise control of the polarization state of the light entering the highly birefringent device. The spectral response was recorded (see Fig. 3). The device shows a narrow full width at half maximum linewidth ( $7 \text{ nm}$  for TE,  $21 \text{ nm}$  for TM) and a resonance spacing of approximately  $21 \text{ nm}$  for TE and  $61.5 \text{ nm}$  for TM in the  $1250\text{--}1360 \text{ nm}$  range. The significant difference between TM and TE resonance spacing is primarily a result of the large material birefringence ( $n_{\text{TE}} = 2.18$  and  $n_{\text{TM}} = 1.60$  at  $\lambda = 1.3 \mu\text{m}$ ). Off-resonance insertion loss was very low ( $<0.5 \text{ dB}$ ), while the extinction ratio on resonance was  $>20 \text{ dB}$  for both TE and Tm polarization. The resonance linewidths are strongly affected by both the surface quality and parallelism of the overlay waveguide. The low device inser-

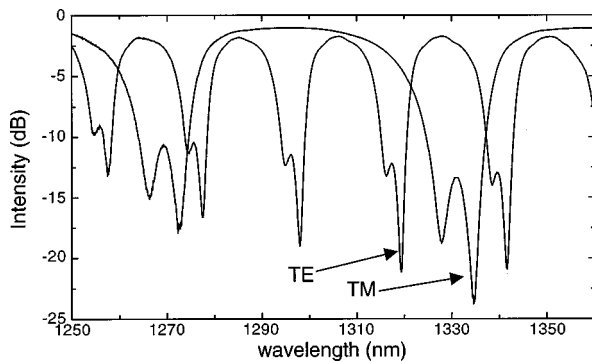


FIG. 3. SPF/DAST<sup>®</sup> C-plate device—spectral response (25  $\mu\text{m}$  thickness, TE and TM polarizations).

tion loss indicates that the DAST<sup>®</sup> surface quality is of fairly good quality and suggests that lack of parallelism is the primary cause of resonance broadening. Thus, enhanced spectral performance can be expected from DAST<sup>®</sup> devices if the waveguide quality can be further improved.

The above SPF/DAST<sup>®</sup> device was configured as an intensity modulator by appropriately aligning a coplanar strip (CPS) electrode pattern on the top surface of the DAST<sup>®</sup> waveguide. The electrode pattern was produced on a polished fused silica substrate so that the requirement for photolithographically patterning the DAST<sup>®</sup> waveguide was avoided. The combined electrode and optical device design allowed a significant component of the applied electric field to act on the large  $r_{11}$  electro-optic component possessed by DAST<sup>®</sup>. Furthermore, it removed any requirement for electrically conductive films above the fiber core region, which would have caused resonance broadening and excess loss. Thus, a refractive index modulation could be achieved with low-power consumption (a low applied voltage) due to the large electro-optic coefficients, high refractive index, and low dielectric constant along the  $x_1$  axis.

Application of an electric field causes the spectral response to shift to higher and lower wavelengths in response to the field orientation. Figure 4 illustrates the intensity modulation mechanism which can be accessed in this device architecture.

The DAST<sup>®</sup> SPF device was placed in a rf optical link and probed with a 1300 nm region narrowline tunable laser. The lasing wavelength was swept through a spectral resonance while a rf signal was applied to the device electrodes. The modulated optical signal was fed into a high-speed photodetector and the output displayed on a rf spectrum ana-

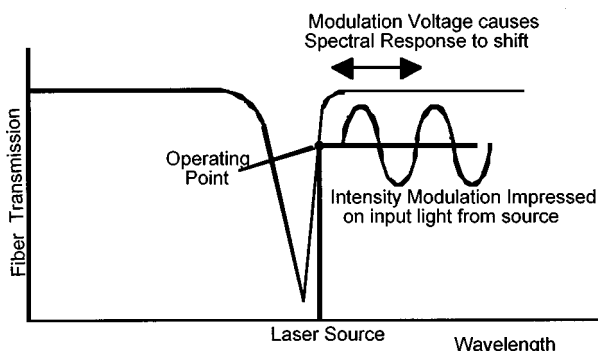


FIG. 4. Intensity modulation technique for SPF/overlay architecture.

lyzer. Optimum modulation sensitivity occurred at a lasing wavelength of 1321.25 nm for TE polarization. The device frequency response was reasonably flat out to 18 GHz (the limit of the test equipment), although modulation sensitivity was fairly low (0.75%/V). Higher modulation sensitivity can be expected from devices with sharper spectral features since the slope of the resonance directly impacts the electrical-to-optical modulation efficiency. It is believed that some of the high-end roll-off in the rf frequency response was primarily due to the application of silver paint for connection to CPS electrodes. Silver epoxy was preferred but required a high-temperature cure, which was not suitable for this particular device generation. Better quality millimeterwave assembly detail should allow the frequency response to extend beyond 100 GHz since the DAST<sup>®</sup> dielectric constant and loss tangent are low, and the device interaction length is short ( $<2$  mm). Such a short interaction length allows for minimal rf and optical velocity mismatch.

In conclusion, single-crystal DAST<sup>®</sup> waveguides with thicknesses in the 20–25  $\mu\text{m}$  range have been successfully fabricated via mechanical polishing technique. The waveguides were investigated via an evanescent coupling technique using side-polished fibers rather than traditional end-firing methods. Surface quality is believed to have been sufficient for low-loss propagation. An intensity modulator was constructed by adding high-speed electrodes to the SPF/DAST<sup>®</sup> overlay architecture. Intensity modulation was observed out to 18 GHz. The device frequency response is believed to extend beyond 100 GHz under optimum conditions.

The authors thank G. Wagoner, B. Lawrence, K. R. Stewart, and M. Shimazu for worthwhile discussions, and K. Chan, P. Quantock, and G. Jameson for their technical assistance. The authors wish to acknowledge partial support by the U.S. DoD under Contract No. MDA904-97-C-3046. DAST<sup>®</sup> is a registered trademark of Molecular OptoElectronics Corp.

<sup>1</sup>K. Noguchi, O. Mitomi, and H. Miyazawa, *J. Lightwave Technol.* **16**, 615 (1998).

<sup>2</sup>D. W. Dolfi and T. R. Ranganath, *Electron. Lett.* **28**, 1197 (1992).

<sup>3</sup>G. K. Gopalakrishnan, C. H. Bulmer, W. K. Burns, R. W. McElhanon, and A. S. Greenblatt, *Electron. Lett.* **28**, 826 (1992).

<sup>4</sup>C. C. Teng, *Appl. Phys. Lett.* **60**, 1538 (1992).

<sup>5</sup>K. K. Loi, L. Shen, H. H. Wieder, and W. S. Chang, *IEEE Photonics Technol. Lett.* **9**, 1229 (1997).

<sup>6</sup>U. Meier, M. Bosch, Ch. Bosshard, F. Pan, and P. Günter, *J. Appl. Phys.* **83**, 3486 (1998).

<sup>7</sup>F. Pan, G. Knöpfle, Ch. Bosshard, F. Follonier, R. Spreiter, M. S. Wong, and P. Günter, *Appl. Phys. Lett.* **69**, 13 (1996).

<sup>8</sup>R. Spreiter, Ch. Bosshard, F. Pan, and P. Günter, *Opt. Lett.* **22**, 564 (1997).

<sup>9</sup>Ch. Bosshard, M.-S. Wong, F. Pan, R. Spreiter, S. Follonier, U. Meier, and P. Günter, in *Electrical and Related Properties of Organic Solids*, edited by R. W. Munn, A. Miniewicz, and B. Kuchta (Kluwer Academic, Dordrecht, 1997), pp. 279–296.

<sup>10</sup>F. Pan, M. S. Wong, C. Bosshard, and P. Günter, *Adv. Mater.* **8**, 591 (1996).

<sup>11</sup>W. Johnstone, S. Murray, M. Gill, A. McDonach, G. Thursby, D. Moodie, and B. Culshaw, *Electron. Lett.* **27**, 894 (1991).

<sup>12</sup>S. Creaney, W. Johnstone, and K. McCallion, *IEEE Photonics Technol. Lett.* **8**, 61 (1996).